

Energy & Environmental Science

Accepted Manuscript



This is an *Accepted Manuscript*, which has been through the Royal Society of Chemistry peer review process and has been accepted for publication.

Accepted Manuscripts are published online shortly after acceptance, before technical editing, formatting and proof reading. Using this free service, authors can make their results available to the community, in citable form, before we publish the edited article. We will replace this *Accepted Manuscript* with the edited and formatted *Advance Article* as soon as it is available.

You can find more information about *Accepted Manuscripts* in the [Information for Authors](#).

Please note that technical editing may introduce minor changes to the text and/or graphics, which may alter content. The journal's standard [Terms & Conditions](#) and the [Ethical guidelines](#) still apply. In no event shall the Royal Society of Chemistry be held responsible for any errors or omissions in this *Accepted Manuscript* or any consequences arising from the use of any information it contains.

COMMUNICATION

Stable electrocatalysts for autonomous photoelectrolysis of hydrobromic acid using single-junction solar cells

Cite this: DOI: 10.1039/x0xx00000x

N. Singh,^a S. Mubeen,^{a,b} J. Lee,^b H. Metiu,^b M. Moskovits,^b and E. W. McFarland^aReceived 00th January 2012,
Accepted 00th January 2012

DOI: 10.1039/x0xx00000x

www.rsc.org/

Metal sulfides that are stable in bromine were investigated as electrocatalysts for hydrogen evolution in a photoelectrochemical device converting HBr to H₂(g) and Br₂(l). The photoanode was stabilized against photocorrosion using a poly(3,4-ethylenedioxythiophene) poly(styrenesulfonate) (PEDOT:PSS) coating. Low loadings of rhodium sulphide nanoparticles were used as cathode electrocatalyst in place of platinum resulting in substantial improvement in the performance of a GaAs-based photosynthetic cell.

Direct solar-to-chemical conversion, artificial photosynthesis, is an attractive and sustainable route to the production of valuable chemicals and fuels that can be used directly, or as energy storage media.^{1,2} Solar photoelectrolysis of hydrogen halides (e.g. HBr) to hydrogen and a halogen (e.g. Br₂) is particularly interesting since the process is electrochemically efficient and the products are valuable.^{3–6} However, the instability of most efficient photoelectrodes in strong acids has impeded the exploitation of this process.

Although the semiconductor anode can be stabilized through the use of protective coatings such as PEDOT:PSS,⁷ there is sufficient crossover of the bromine produced to corrode and poison most hydrogen evolution cathode materials (e.g. platinum). The development of hydrogen evolution electrocatalysts that are stable in the halogen/halide electrolyte is crucial for this solar-to-chemical system to be useful. Of course metal electrocatalyst films (such as those of platinum/iridium) can be made thick enough to allow long catalyst life.⁴ This, however, is a costly solution that also reduces light collection due to reduced transparency. Clearly, a catalyst consisting of dispersed nanoparticles is desirable, but unfortunately platinum group metals are not stable as nanoparticles in halogen/halide electrolytes.^{8,9} A number of metal sulfides might be good candidate materials since they

have been shown to be stable as oxygen depolarized cathodes for chlorine production from hydrochloric acid^{10–14} and as hydrogen evolution cathodes for the electrolysis of HBr.¹⁵

In this communication we demonstrate the advantage of rhodium sulfides as a cathode electrocatalyst in a photoelectrochemical device consisting of a single-junction gallium arsenide (GaAs) cell that photoelectrochemically electrolyzes HBr with simulated sunlight as the only energy input. This work shows how the design of a stabilized electrocatalyst coating can facilitate the use of a high efficiency buried semiconductor junction which would otherwise corrode in most useful electrolytes.

To examine the stability of a cathode electrocatalyst in a Br⁻/Br₃⁻ environment, cyclic voltammograms (CV) were measured in fuming HBr (Figure 1). For the initial cycles (≤5), both Pt/C and Rh_xS_y/C electrodes prepared on ITO using a Nafion binder (see Electronic Supporting Information for details) exhibited a strong catalytic wave with hydrogen evolution onset at -0.1 V vs. Ag/AgCl electrode. However as the number of cycles increased, hydrogen evolution at the Pt/C surface decreased, with no detectable currents after 360 cycles (Figure 1a). We speculate that the rapid decrease from 350 to 360 cycles is because the Pt catalyst is continuously corroded but not limiting current until approximately 350 cycles when the last remnants of the Pt are still available. At approximately 350 cycles the last of the catalyst is removed and the activity drops to zero (by 360 cycles). The electrochemical stability of Pt films or Pt/C as a hydrogen evolution electrocatalyst for HBr electrolysis is likely limited by the instability of the nanoparticulate Pt in the presence of Br⁻/Br₃⁻. This is believed to be due Br⁻ binding to the Pt, blocking active sites,^{16,17} and the dissolution of Pt in the presence of Br₃⁻, which forms through the reaction of Br⁻ with bromine. Although a membrane can be used to block Br₃⁻ transport, crossover can still occur, allowing the bromine that is formed on the counter electrode to corrode the Pt/C. In contrast, the activity of an electrode in which the Pt/C catalyst was replaced with Rh_xS_y/C remains constant after a small initial

decrease, as shown in Figure 1b in which the stability of the Rh_xS_y is compared to that of Pt. A possible reason for the initial decrease in activity for $\text{Rh}_x\text{S}_y/\text{C}$ is desorption of physically adsorbed catalyst due to insufficient Nafion binder. The procedure used was optimized for deposition of catalysts onto a glassy carbon electrode, and further optimization may be helpful in improving the adsorption of the catalyst on a PEDOT:PSS coated surface. It is also possible that Br^- reduces the Rh_xS_y activity rapidly to a lower, but stable steady-state activity. The mechanism for the decreased anodic current for the $\text{Rh}_x\text{S}_y/\text{C}$ catalyst after several scans is unclear and merits further investigation.

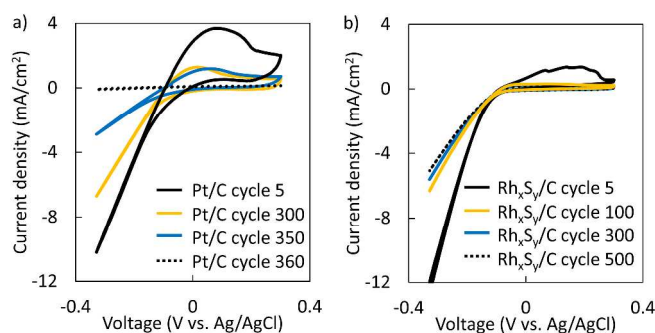


Figure 1: Cyclic voltammograms showing hydrogen evolution using a) Pt/C and b) $\text{Rh}_x\text{S}_y/\text{C}$ both deposited on an ITO electrode from inks. The scan rate was 20 mV/s, with Ag/AgCl reference electrode and Pt counter electrode. The electrolyte was fuming HBr with no separator between counter and working electrode. The $\text{Rh}_x\text{S}_y/\text{C}$ reaches a stable HER activity, while with time the Pt/C corrodes and the activity is severely reduced.

The stability of the sulfide catalyst is also demonstrated by the minimal dissolution of Rh_xS_y after exposure of the catalyst to 6 M HBr, 6M HCl and 6M HClO_4 for two weeks (Table 1). In addition, the crystallinity of $\text{Rh}_x\text{S}_y/\text{C}$ measured by X-ray diffraction did not change after 4 hours of continuous cycling in fuming HBr. The stability of the Rh_xS_y electrocatalyst makes it an excellent (and cost effective) replacement as the hydrogen evolution electrocatalyst for photoelectrolysis of HBr. Although rhodium is expensive, the metal loading used in the photocathode is extremely low, 0.0432 mg/cm² (the same loading of metal would be made by a 35 nm thick film of Rh, or 20 nm of Pt). The cost is approximately \$20/m² for either metal, which for a 10% efficient system would equal ~\$0.20/W_{peak}. (See ESI for discussion).

Table 1. Percentage of Rh dissolved after exposure to 6M HBr, HCl, HClO_4 for two weeks

Acid	Rh dissolved (%)
HBr	2.1 ± 0.2
HCl	4.7 ± 0.2
HClO_4	2.9 ± 0.2

The solid state IV curve under illumination for a commercial p-n GaAs cell is known, allowing it to be compared in the same plot with I-V performance data from the electrocatalysts used in a photoelectrochemical device. To compare to conditions in a PEC device, the electrocatalysts are oriented facing away from one another and have the same area as the final cell to be tested, thus accounting for any mass transfer limitations within the cell. The predicted operating photocurrent and voltage of an autonomous

photoelectrochemical system consisting of a p-n junction with electrocatalysts deposited on both the anode and the cathode, are given by the intersection of the solid-state semiconductor IV curve and the electrochemical current-voltage relation of the electrocatalysts deposited on the semiconductor device faces (Figure 2a).¹⁸

After the electrocatalysts have been applied onto the semiconductor anode and cathode, the operating current density of the device under illumination was measured by the rate of hydrogen gas evolution (using a gas chromatograph). The initial rate is consistent with the current density calculated by the solid state IV measurement of the GaAs device and the catalyst IV curve (Figure 2b).

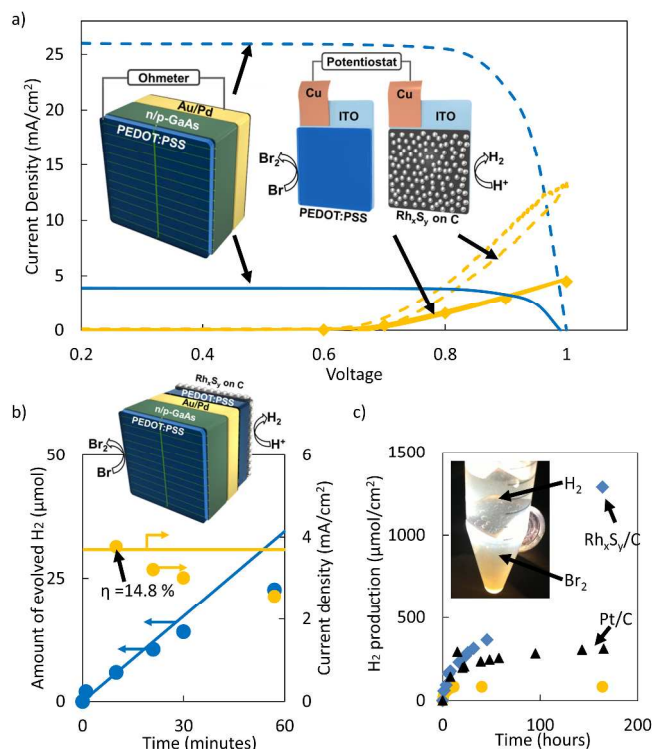


Figure 2: a) The current and voltage relationships of: two-electrode system using a $\text{Rh}_x\text{S}_y/\text{C}$ on PEDOT cathode and PEDOT anode in 48wt% HBr as an uncompensated (solid orange line) and IR compensated (dotted orange line) cyclic voltammogram, and 10 minute averaged constant potential (orange dots) compared with the solid state IV curve for a commercial GaAs single junction cell under 100 mW/cm² illumination (blue dotted line) and 15 mW/cm² (blue line), the schematics of the two-electrode system and the solid state solar cell measurement are shown in the inset. b) gas chromatography measured hydrogen production (blue dots), corresponding current density (orange dots) for the GaAs with $\text{Rh}_x\text{S}_y/\text{C}$ cathode electrocatalyst depicted in (a), and hydrogen production (blue line) and current density (orange line) predicted by the intersection of the solid state IV measurement of the GaAs device and the electrochemical IV curve of HBr electrolysis. The electrolyte was 8.4 M HBr and the illumination was 15 mW/cm². The efficiency is obtained from the starting open circuit voltage in the electrolyte (0.6 V) multiplied by the current density divided by the illumination (15 mW/cm²). The schematic of the wireless system is shown in the inset of b). c) hydrogen production rate showing long-term stability of the overall device, due to the use of the stable Rh_xS_y catalyst instead of Pt. Samples are non-O₂ plasma etched before PEDOT:PSS deposition with $\text{Rh}_x\text{S}_y/\text{C}$ on the cathode (blue) or Pt/C (black). These samples were illuminated by 60 mW/cm² and the overall efficiency after 164 hours of operation was 0.4% for the $\text{Rh}_x\text{S}_y/\text{C}$ sample (blue). The system under operation is shown in the inset of (c), with

hydrogen forming at the top (cathode) and bromine collecting after forming at the bottom (anode).

The initial efficiency of the best performing device, at 15 mW/cm² illumination, was 14.8%. The use of Rh_xS_y instead of Pt extends the device lifetime (Figure 2c), because the poisoning/corrosion of the electrocatalyst does not inhibit the production of hydrogen. Transmission electron microscopy images (Figure S3) did not show significant change in the structure of the catalyst and by energy dispersive x-ray spectroscopy no significant changes in Rh-S stoichiometry were observed (see ESI). Corrosion was observed on areas of the device that were not completely coated in PEDOT:PSS at the anode, which lead to decreases in the efficiency of the device due to the decreased active area of GaAs. Reloading the Rh_xS_y/C catalyst did not, however, greatly improve the H₂ production of the device suggesting that, for the GaAs/Rh_xS_y system, factors other than the cathode electrocatalyst are responsible for the decrease in efficiency with time (Figure S8). The overall efficiency of the device after 100 hours was 1.2% when illuminated at 15 mW/cm², (Figure S9) and 0.4% at 60 mW/cm² for 164 hours.

Following sustained production of bromine and hydrogen, the back reaction of bromine reduction to bromide ions resulted in a decrease in the Faradaic efficiency of the hydrogen evolution reaction, which might account for the drop in hydrogen production. A potential solution would be to place a membrane onto the cathode electrocatalyst, or to complex the bromine molecules with an agent such as polyethylene glycol¹⁹ to reduce the quantity of bromine present at the cathode. Additionally, supporting the Rh_xS_y on a material that is unreactive in the bromine back reaction (in place of carbon) may improve the selectivity for hydrogen production. However, replenishing the solution with fresh HBr, thus reducing the amount of Br₂ present produced only a minimal increase in efficiency. Also, PEDOT:PSS did not fully coat the GaAs anode unless an O₂ plasma etching step was used on the GaAs, resulting in much lower rates of H₂ evolution after ~12 hours of operation as shown in Figure 2c.

The effect of exposure to 3M HBr on the surface composition of Rh_xS_y/C is shown by XPS characterization (Figure 3a and b).

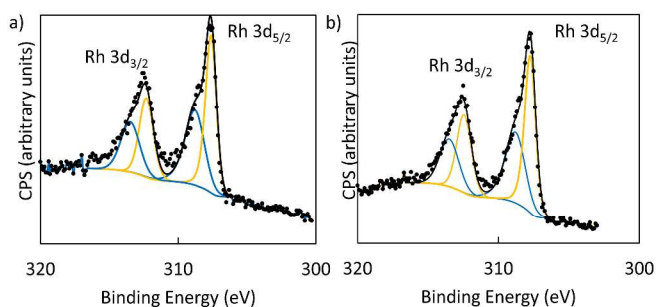


Figure 3: High resolution XPS scan for a) as prepared and b) HBr exposed Rh_xS_y/C for Rh. The raw data is in black dots. The data was fitted to a peak (black curve) using a combination of the orange (307.7 eV Rh 3d_{5/2} peak) and blue (308.8 eV

Rh3d_{5/2}) peaks and the ratio of their areas was used for comparison of Rh oxidation states.

The ratio of oxidation states of Rh measured by the Rh 3d binding energy was relatively unchanged by exposure to HBr: 1) 1.19:1 of 307.6 eV:308.8 eV Rh(IV) prior to exposure of HBr, and 2) 1.25:1 of 307.7:308.8 eV Rh(IV) after exposure to HBr. The 308.8 eV peak may correspond to Rh(IV),²⁰ and 307.7 eV peak may correspond to a slightly oxidized Rh species. The XPS observed concentration of Rh at the surface (Figure S10), did not vary significantly, consistent with the electrochemical and chemical stability shown in Figure 1. Full XPS survey scans and high resolution scans are shown in Figure S10-13.

In conclusion, a GaAs based photoelectrochemical device was stabilized for an HBr environment by coating the anode with PEDOT:PSS and activating the cathode side for hydrogen production with a Rh_xS_y hydrogen evolution electrocatalyst dispersed on carbon using a Nafion binder. The free-standing device structure under illumination produced hydrogen and bromine without external bias or any other electrical connections for over 150 hours in fuming HBr. This performance far exceeds that of a Pt cathode electrocatalyst. The structure and processing steps may be used with most high efficiency semiconductors suggesting that efficient and stable electrocatalysts may be developed for numerous light absorbers, including such otherwise unstable semiconductors as chalcogenides and phosphides that, as a result, may be used for efficient as well as durable solar photoelectrocatalysis.

Acknowledgements

N. S. is supported by the ConvEne IGERT Program (NSF-DGE 0801627). Tom Mates assisted with XPS measurements. This work was partially supported by the MRSEC Program of the National Science Foundation under Award No. DMR 1121053. Helpful discussions with Shane Ardo are greatly appreciated.

Notes and references

^a Department of Chemical Engineering, University of California, Santa Barbara, USA

^b Department of Chemistry and Biochemistry, University of California, Santa Barbara, USA

Electronic Supplementary Information (ESI) available: Experimental details and additional figures. See DOI: 10.1039/c000000x/

1. M. D. Archer, *J. Appl. Electrochem.*, 1975, **5**, 17.
2. K. Rajeshwar, P. Singh, and J. DuBow, *Electrochim. Acta*, 1978, **23**, 1117.
3. J. D. Luttmer and I. Trachtenberg, *J. Electrochem. Soc.*, 1985, **132**, 1820.

4. J. Luttmer, D. Konrad, and I. Trachtenberg, *J. Electrochem. Soc.*, 2001, **26**, 127.
1985, **132**, 1054.
5. W. McKee, *IEEE Trans. Components, Hybrids, Manuf. Technol.*, 1982, **5**, 336.
6. *US Pat.*, 4 021 323, 1977.
7. S. Mubeen, J. Lee, N. Singh, M. Moskovits, and E. W. McFarland, *Energy Environ. Sci.*, 2013, **6**, 1633.
8. G. H. Schuetz and P. J. Fiebelmann, *Int. J. Hydrogen Energy*, 1980, **5**, 305.
9. T. Van Nguyen, H. Kreutzer, V. Yarlagadda, E. McFarland, and N. Singh, *ECS Trans.*, 2013, **53**, 75.
10. J. M. Ziegelbauer, A. F. Gullá, C. O'Laoire, C. Urgeghe, R. J. Allen, and S. Mukerjee, *Electrochim. Acta*, 2007, **52**, 6282.
11. J. M. Ziegelbauer, D. Gatewood, A. F. Gullá, M. J. Guinel, F. Ernst, D. E. Ramaker, and S. Mukerjee, *J. Phys. Chem. C*, 2009, **113**, 6955.
12. A. F. Gullá, L. Gancs, R. J. Allen, and S. Mukerjee, *Appl. Catal. A Gen.*, 2007, **326**, 227.
13. J. Ziegelbauer, V. Murthi, C. Olaoire, A. Gullá, and S. Mukerjee, *Electrochim. Acta*, 2008, **53**, 5587.
14. J. M. Ziegelbauer, D. Gatewood, S. Mukerjee, and D. E. Ramaker, *ECS Trans.*, 2006, **1**, 119.
15. A. Ivanovskaya, N. Singh, R.-F. Liu, H. Kreutzer, J. Baltrusaitis, T. Van Nguyen, H. Metiu, and E. McFarland, *Langmuir*, 2013, **29**, 480.
16. V. Livshits, A. Ulus, and E. Peled, *Electrochem. commun.*, 2006, **8**, 1358.
17. J. Orts, R. Gómez, and J. . Feliu, *J. Electroanal. Chem.*, 1999, **467**, 11.
18. O. Khaselev, A. Bansal, and J. A. Turner, *Int. J. Hydrogen Energy*, 2001, **26**, 127.
19. L. A. Kosek J., *Investigation of bromine complexed hydrogen/bromine regenerative fuel cells for portable electric power*, MERDC-38, 1984.
20. Y. Abe, *Surf. Sci. Spectra*, 2001, **8**, 117.